

Power Lines and Catastrophic Wildland Fire in Southern California

Joseph W. Mitchell^a

ABSTRACT

In October 2007, Southern California was hit by multiple simultaneous catastrophic fires driven by “Santa Ana” Foehn winds. Half of these fires – the largest and most destructive – have been attributed to power lines. Comparing scaling relations for historical fire sizes demonstrates that power line fires tend to be larger than wildland fires from other sources. This occurs because the number of line faults rise rapidly as a function of wind speed while fire suppression efficiency drops from its usual 99% to around 80% under high-wind conditions. Three physical effects causing power line fires – tree contact, line slap, and metal fatigue – are shown to lead to a number of ignitions that increase at least as wind speed squared, and probably as a much stronger function of wind speed. Current regulations are shown to be inadequate to protect against extreme wind events, making the reoccurrence of power line conflagrations equalling or worse than that of October 2007 inevitable barring significant additional preventative measures to be taken by utilities and regulators.

POWER LINE WILDLAND FIRES IN SOUTHERN CALIFORNIA

Fire records maintained by the California Department of Forestry and Fire Protection (“Cal Fire”) show that power lines are currently responsible for about 3% of all ignitions within their jurisdiction in California¹. However, power lines ignited four of the twenty largest fires in California history by acreage and four or five of the twenty largest fires by structures destroyed². The probability that a rate of 3% would produce a fluctuation resulting in an observation of 4 or more out of 20 events is only 0.3% - strongly suggesting that power line fires are somehow larger than fires started by other means.

The causal mechanisms responsible for making power line fires larger and more destructive than fires from other ignition sources has long been understood, though not fully quantified, by fire agencies and utilities. A collaborative effort between Southern Californian power companies and fire agencies produced a “Power Line Fire Prevention Field Guide” in 2001, which astutely notes the reasons that power lines present an extraordinary hazard:

“The potential exists that power line caused fires will become conflagrations during the long hot and dry fire season commonly experienced in California. The very same weather conditions that contribute to power line faults also lead and contribute to the rapid spread of wildfire. The most critical of these weather factors is high wind, which is commonly accompanied by high temperatures and low humidity.”³

This causal linkage – wind causing faults and the ejection of hot materials which cause the ignition of wildland fuels and the subsequent rapid growth of the fire due to wind – is the reason that power line fires tend to be larger than those from other ignition sources. This effect can be observed in fire perimeter data released as part of Cal Fire’s FRAP (Fire and Resource

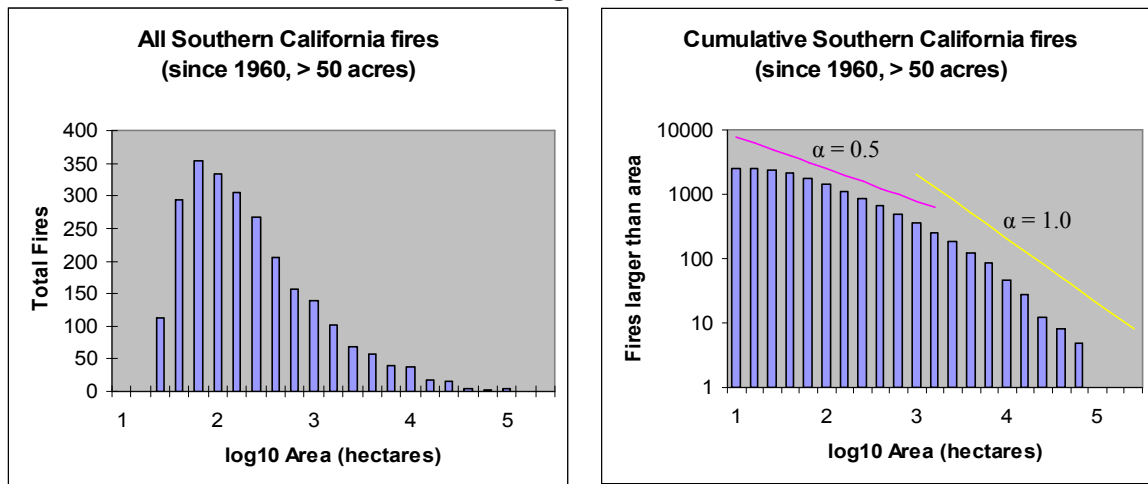
^a M-bar Technologies and Consulting, LLC, Ramona, CA; 19412 Kimball Valley Rd., Ramona, CA 92065; jwmitchell@mbartek.com

Assessment Program) project.⁴ This data set represents historical fire perimeters extending back almost a century obtained from Cal Fire records as well as those of the US Forest Service, the US Bureau of Land Management, and the National Parks Service. While threshold for collection is 50 acres for brush fires, 10 acres for timber fires, and 300 acres for grass fires, these are not always strictly adhered to. Also, some inaccuracies were noted in the dataset during analysis and reported to Cal Fire, which implies that remaining low-level error exists in the data set. However, this collection remains the only comprehensive data set providing geographical and other information on fires in all of California, and errors should have a minor statistical impact.

Size distributions for forest fires have been shown to follow power-law distributions, which is to be expected for self-organized criticality⁵. Moritz et al.⁶ have applied a Highly Optimized Tolerance (HOT)⁷ model (specifically a Probability Loss Resource, or PLR model) to fire regimes in a variety of fire landscapes, and find excellent agreement for a model assuming two dimensional fire regions constrained by one dimensional constraining perimeters where fires are extinguished by either fire breaks or the application of fire suppression resources. The approximate solution to this problem is characterized by a power law distribution with critical exponent $\alpha = 1/d = 0.5$, with a lower constraint C and an upper constraint L : $P(l) = A((C+l)^{-\alpha} - (C+L)^{-\alpha})$.

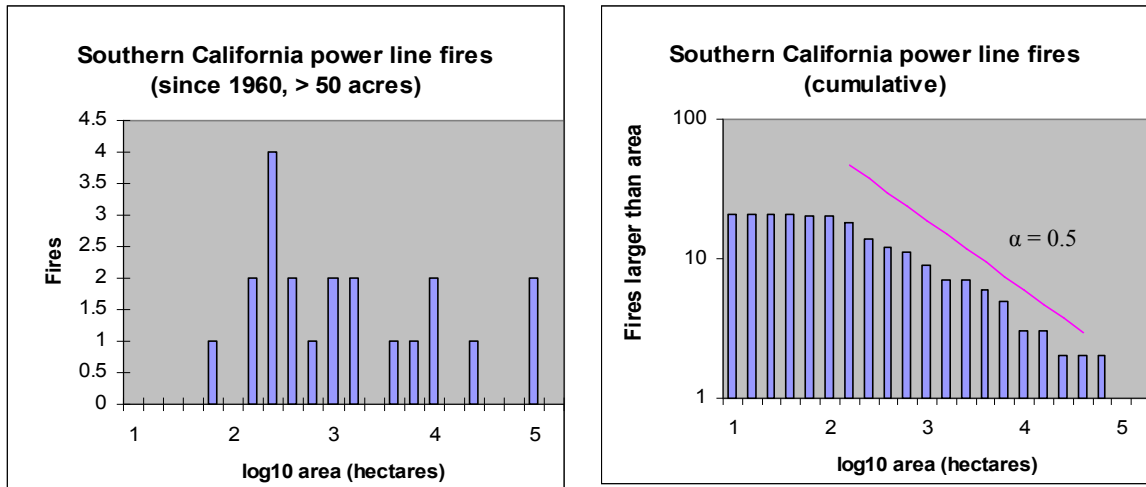
Restricting the FRAP dataset to Southern California only (the counties of San Diego, Orange, Riverside, San Bernardino, Los Angeles, and Ventura), and to fires after 1960, the data contains records of 2,523 fires larger than 50 acres, as shown in Figure 1. Exponential curves with a slope of 0.5 and 1.0 are shown, and comparison indicates that size scaling does not follow a simple power law distribution, but falls off more steeply at larger fire sizes.

Figure 1



Fire causes are identified in the data set, and those fires attributed by Cal Fire to power lines are shown in the size distribution plot in Figure 2:

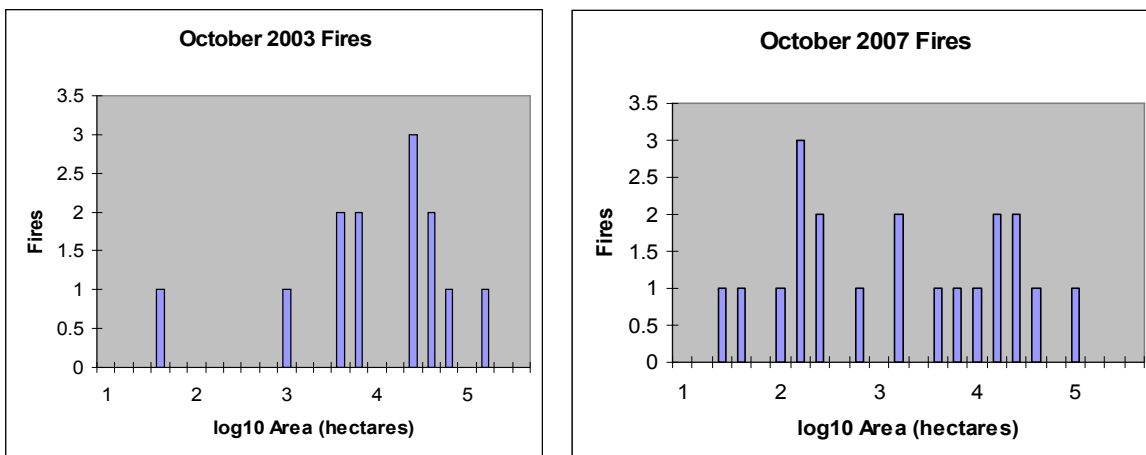
Figure 2



The size distribution of power line fires in Southern California, shown as raw and cumulative plots. An exponent of -0.5 is plotted for comparison.

It is clear that the size distribution for fires started by power lines and fires from other sources are different, with power line fires tending to have a larger size. The underlying mechanism that explains this difference seems to be that power line fires are more likely to occur under conditions of high wind. Figure 3 shows size distributions for fires in the data set from all sources that started during two extended periods of high wind – one in October 2003 and the other in October 2007. Note that the shape is similar to that of power line fire events^b.

Figure 3



Size distribution of fires started during the Santa Ana weather conditions of October 2003 and October 2007 are plotted.

In the Probability-Loss-Resource model of Carson and Doyle, it was observed that

^b Power line events exist in the October 2007 sample, but have a similar size distribution to other events.

wildland fires in California showed a size scaling with an asymptotic scaling exponent of $\alpha = -1.0$ while other wildland fire sets had an exponent of $\alpha = -0.5$. This was generalized to even more wildland fire data sets in Moritz et al. The reason suggested by Carson and Doyle for the more rapid drop off with size in the California data set is the roughness of the California terrain, which they assert might lead to lower fractal dimensions of the landscape and hence steeper power laws.

An alternative interpretation is offered by the work of Boer et al.⁸ They note that the scaling exponent for a number of Australian fire regions varied between -0.32 and -0.62, and that this variation correlates with the magnitude of weather events for a considerable portion of the size interval. They argue for external forcing, rather than endogenous effects, is the mechanism determining the scaling exponent.

The high-wind and power line distributions shown above take place on the same terrain as the Southern California fire set used by Moritz et al., but exhibits a much slower drop-off with increasing size. The simple PLR model used by Carson and Doyle, however, assumes constant resource availability, where “resources” are efforts to create firebreaks. However, what constitutes a “firebreak” depends on external variables, such as wind speed, since firebrands can be transported for great distances during catastrophic fire events^{9,10,11,12}. Hence, we would expect resources to “disappear” as wind speed increases. As far as resources supplied by firefighting, these 1) become more limited as resources are spread thinly due to multiple fire events and 2) are not able to effectively deploy as effectively due to the rapidity of fire growth. These effects are equivalent to an increase in scale of the landscape, with an effective relative decrease in the available resources per unit area. Hence, we should not expect a simple PLR model with static firebreaks to be representative, and we expect the characteristic sizes of fires to become larger with increasing wind speed, with a corresponding decrease in the slope. This effect would also explain the weather-dependent scaling observed by Boer et al. The effectiveness of fire suppression under high-wind conditions is discussed in the next section.

WIND AND WILDLAND FIRES IN SOUTHERN CALIFORNIA

While Southern California is widely known for its catastrophic wildland fires, the vast majority of fires are actively and effectively suppressed prior to their becoming unmanageable. California has an extremely large area of wildland-urban interface, and along with its increasing population in this interface comes an increasing number of human-induced ignitions¹³, which represent the majority of ignitions in this region. While it is known that it is harder for fire agencies to suppress fires during “fire weather”, this effect has not yet been quantified in literature.

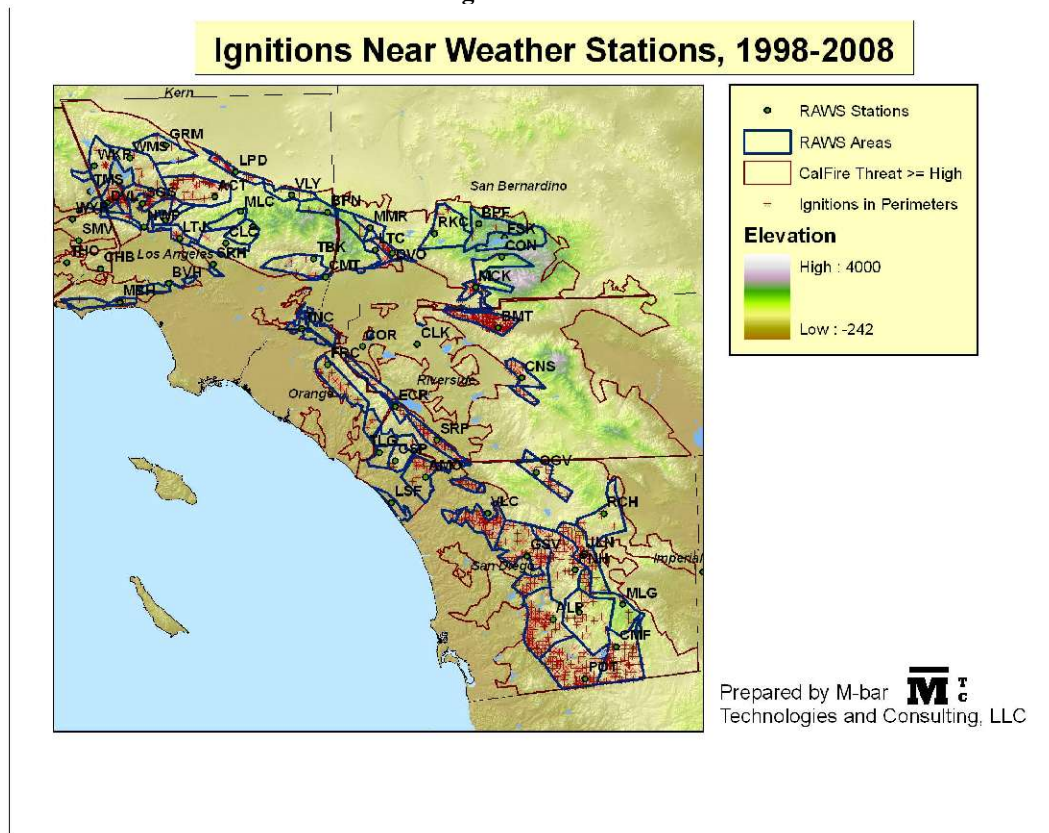
Cal Fire has been collecting ignition data for ignitions and the resulting fires within its own service area and for cooperating agencies since 1998¹⁴. While it is not a complete set, and while it is not possible to vouch for unbiased or accurate collection of data from all agencies in all circumstances, it can be used to make some general observations regarding the effectiveness of fire suppression throughout Southern California during the last decade.

The inclusion of fire sizes allows effectiveness of fire suppression to be determined. For the purposes of this paper, “effective” suppression will be defined as fire size less than 100 acres (40.5 hectares). The counties included in this study include San Diego, Orange, Riverside, San Bernardino, and Los Angeles. No data was available for Ventura County. There were a total of 19,715 recorded ignitions in this data set, with only 231 exceeding the “effective suppression” limit in size, for a suppression rate of $98.8 \pm 0.1\%$.

In order to study the effect of “fire weather” and wind on fire suppression, it is necessary to have a relevant measurement of wind speed at the point and time of ignition. The landscape of California is varied, and wind velocities tend to vary strongly with elevation, topology, aspect, and geographical location. In particular, the “Santa Ana” winds of Southern California tend to have a specific direction (easterly or north, depending on geographical location), and vary strongly with elevation and distance from the sea and its countervailing on-shore winds¹⁵. Hence, it is likely that wind predictions for a given geographic point will be most accurate if they are based on measurements at a station in a proximate location and in a region of similar elevation, slope, and aspect.

The US Forest service operates a network of Remote Automated Weather Stations (RAWS)¹⁶ throughout California. Areas around these stations in the southern California study area were chosen having similar elevation and aspect. In order to guarantee that only ignitions occurring in suitable fuel conditions were included in the sample, a further cut was placed on the ignition data by requiring that the areas be within a perimeter within which the predominant wildland fire threat rating by Cal Fire¹⁷ was “High” or greater. A map of the areas assigned to each station and the ignitions within that area are shown in **Error! Reference source not found.**

Figure 4



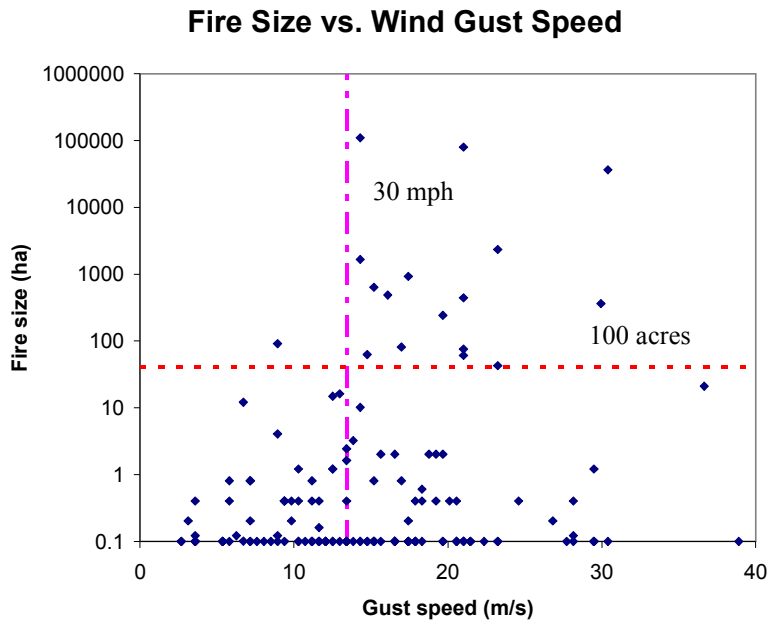
The total number of ignitions within areas having high ignition potential and falling within the area defined for the selected RAWS stations was 2,333. There were 66 of these fires that exceeded the 40.5 ha threshold, giving a suppression rate of $97.2 \pm 0.3\%$. When only fires occurring during the September to March Santa Ana season are included, 34 ignitions out of 802

exceeded threshold, for a suppression rate of $95.8 \pm 0.7\%$.

The criteria used for determining whether an ignition occurred during “Santa Ana” conditions were that the relative humidity be less than 30% for over 80% of the measurements for a period equal or greater than 24 hours, and that the wind trend from the east or north (depending on station) during this period. The RAWS wind data for each station were obtained from the Mesowest collaboration website¹⁸, where historical data is available in graphical form. Applying this selection, 158 events were observed, 17 of which were larger than the selection criterion of 40.2 ha, giving a suppression efficiency of $89.2 \pm 2.6\%$. The maximum wind gust speed in a period extending from two hours before the ignition event to twelve hours after the ignition was recorded from the Mesowest graphs and is plotted in Figure 5.

The effective suppression limit of 40.2 ha (100 acres) is indicated by the horizontal dashed line. What is most evident from this graph is the presence of a threshold at 13.4 m/sec (30 mph) above which almost all fires exceeding the effective suppression limit occur. Above the gust speed threshold, there were 16 events larger than the suppression limit out of 83 total events, for a suppression efficiency of $80.3 \pm 4.8\%$. The statistical significance of this threshold is $p = 0.016$ ($\chi^2 = 5.77$, DOF =1). Above this threshold, however, no significant correlation between maximum gust speed and size is observed ($r = 0.19$). This is counterintuitive, and might suggest that wind conditions at the ignition location may be highly dependent on local topology and conditions and therefore not strongly correlated with the nearest RAWS weather station.

Figure 5



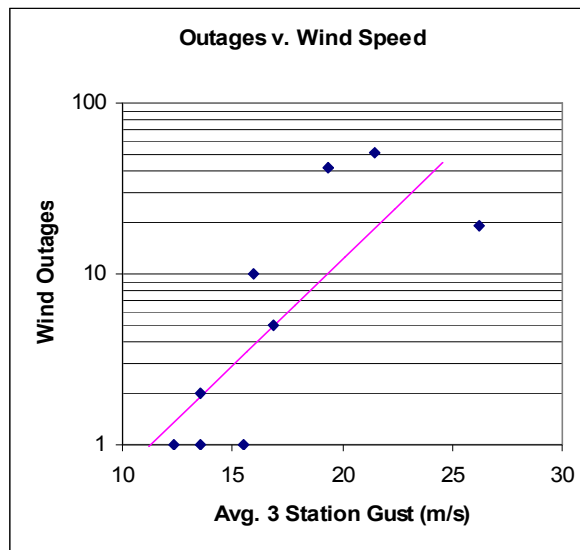
WIND AND POWER LINE IGNITIONS

Fires starting under high-wind conditions have been shown above to be larger than fires starting in calm conditions, even when including other weather variables such as relative humidity. The tendency of power line fires to become more frequent during extreme events, such as in October 2007 when they were responsible for up to nine of 20 major fires, is due to the fact

that the ignition probability rises under high-wind conditions as well.

As part of an application process for a new transmission line, San Diego Gas & Electric Company (SDG&E) supplied both fire and outage data that was subsequently used in testimony before the California Public Utilities Commission(CPUC)¹⁹. Outage data were for transmission lines only (69 kV and above), and not distribution lines, spanning the period from 1998 through 2007. It was observed that these outages came in time-correlated clusters, and the size of these clusters was analyzed to determine the correlation with wind speed. The outage data itself flagged some of the outages as related to high winds. There were 15 events meeting this criterion. No geographical information was made available for these outages, so in order to determine a corresponding wind speed the maximum wind gust data from three RAWS stations (Julian, Potrero, and Ammo Dump) within a 12 hour window on either side of the outage cluster were obtained graphically from Mesowest and averaged. Not all stations were operable for all data points and only those points having data for all three stations were included in the sample, leaving nine wind-induced events. These are plotted in lines, is summarized in Table 1: .

Figure 6 – Outages vs. Wind Speed



The obvious threshold of around 13 m/s (30 mph) in wind gust speed is perhaps due to the fact that wind would not be recorded as a contributing factor otherwise. A correlation between wind speed and number of outages, however, is clear. It should be pointed out that statistically significant clusters of three or more outages occur that are not correlated with wind. Twenty of these clusters between 1999 and 2006 were scanned to see if any wind-induced events were unreported, and only one with a wind speed above 30 mph was found. These other outage clusters are likely due to electrical issues and not to wind events²⁰.

Not all electrical faults in a transmission network would be expected to cause fires. However, we would generally expect fires caused by or associated with a power line to either cause or be caused by a line outage. Since 2004, SDG&E has collected power line fire data, and data from 2004 to 2007 were also presented during the CPUC hearings by participating parties²¹. Data for affected lines, both distribution and transmission lines, is summarized in Table 1:

Table 1 - SDG&E Power Line Fires

Distribution - Failure/Wind/Tree	75
Distribution - Human/Bird	33
69/138 kV - Human/Bird	6
69/138 kV - Failure/Wind	4
230 kV - Failure/Wind	2
230 kV – Human	1
500 kV	0

This summary differentiates between fires caused by human activity or animals from mechanical failures, tree contact, or other causes potentially (or actually observed to be) exacerbated by wind. Of the above fires, four were larger than 100 acres: The Open fire of December 2006 (D), and the Witch (T, 69kV), Guejito (D) and Rice (D) fires of October 2007. We can judge the relative fire rates for various line types by normalizing the fire rate for Failure/Tree/Wind fires in the table above to the length of line in the network, as shown in the table below:

Line Type	Length (km)	Rate (yr ⁻¹ km ⁻¹)	Low 90%CL	High 90%CL
Distribution	10879	1.84E-03	1.50E-03	2.23E-03
69 kV + 138 kV	1860	5.74E-04	1.96E-04	1.30E-03
230 kV	623	8.57E-04	1.54E-04	2.70E-03
500 kV	97	--	--	6.33E-03

The normalized rates in fires per kilometer per year and their high and low 90% confidence levels assuming Poisson statistics are plotted above. Uncertainties are large due to the limited statistics available and systematic uncertainties (for instance it was not revealed to what degree each line type is exposed to flammable vegetation, except for the 500 kV segment), but there is an indication that distribution lines have a higher associated fire rate than transmission lines.

INCREASE OF IGNITIONS WITH WIND SPEED

There are a number of mechanisms that are responsible for wildland fire ignitions. All of them to exhibit a stronger than linear behavior with respect to increasing number of ignitions versus wind speed. These mechanisms fall into two distinct categories: those caused by deformation of flexible objects under wind stress (tree limbs, other conductors, etc.) which leads to contact with a conductor and the subsequent ejection of hot materials. For instance, “line slap” of parallel conductors has been shown to be able to cause ejection of hot metal capable of igniting surrounding vegetation²². Another cause of power line faults and subsequent ignitions is fatigue failure of power infrastructure components or of other objects near the conductors.

Wind loading by aerodynamic drag can be expected to vary as the square of wind velocity, \bar{u} ²³,

$$\bar{F}_d = \frac{1}{2} C_d \rho_{air} A |\bar{u}| \bar{u} \quad [1]$$

All variables are defined in the Appendix. Regulatory design requirements for wind loadings in California²⁴ are specified as 383 Pa (8 lb/ft²) for cylindrical objects and 622 Pa (13 lb/ft²) for flat objects below 914 m (3000 ft) elevation and 287 Pa (6 lb/ft²) for cylindrical objects and 479 Pa (10 lb/ft²) for flat objects above (3000 ft) elevation (also includes ice loading), in addition to a component-dependent safety factor. In the range of object sizes ($\gg 1$ cm) and wind speeds of relevance, the drag coefficient is a weak function of wind speed, and the wind speeds corresponding to the design pressures are approximately 20 m/s (44 mph) in the high elevation region and 23 m/s (51 mph) in the low elevation region. As illustrated in Figure 5 and Figure 6, Santa Ana winds speeds can exceed these values.

Elastic extension and conductor contact

One mechanism that can lead to objects contacting conductors is if an object near a conductor flexes elastically in the wind and makes contact with it. For many structures and objects, the flexure will follow Hooke's Law $F = -kx$, where k is the elastic coefficient. Where the external object acts as a torsion spring, the relation is $F = -k\theta$, and for small θ these expressions are effectively the same. In California, a minimum separation between conductors is required and is generally greater than 0.9m (36 in) from other conductors, with specified separation increasing with line tension up to 4 m (156 in) for transmission lines above 300 kV²⁵. Vegetation and tree clearances are less stringent, with the minimum separation being 0.46 m (18 in) for distribution lines and $\frac{1}{4}$ of the pin spacing for transmission lines (up to 0.95 m [38 in] for transmission lines above 300 kV)²⁶.

One would expect that application of a cleared distance around the conductors, combined with routine maintenance would result in a threshold velocity u_{min} below which no conductor-object contacts are observed, and a corresponding minimum elastic constant k_{min} . As the wind speed increases, smaller values of k will be enabled to make line-conductor contact. Assuming that the values of k are evenly distributed, we can derive^c the following relation for number line contacts:

$$N = \frac{B_N L K}{d} (u^2 - u_{min}^2) \quad [2]$$

where B_N is a constant subsuming the aerodynamic drag and geometric constants, K is a constant describing the distribution of elastic coefficients, and u_{min} is the velocity at which an object with spring constant k_{min} will extend a distance d .

Line slap

“Line slap” occurs when parallel conductors contact each other or other components under windy conditions. This is accompanied by arcing and the ejection of hot metal particles that can be an ignition source²⁷. It can occur when the horizontal line sag under load exceeds one half the conductor separation. Regulatory requirements state that line tension under design wind load must be less than the tensile strength of the cable by a safety factor, equal to two for conductors, which can result in significant sag for long segments. For instance, a bare copper conductor cable with commonly used diameters and 100 m. in length will exhibit at least 0.9 m (3 feet) of sag²⁸. The ratio of horizontal sag due to wind drag compared to vertical sag due to gravity varies as a function of conductor material and diameter as well as wind speed. At the maximum design wind pressure of 290 Pa (6 lb/in²), horizontal and vertical sag will be equal for ACSR (aluminium conductor steel reinforced) cables 2.0 cm in diameter, stranded copper cable 1.3 cm in diameter,

^c See Appendix for derivation.

copper covered steel 0.8 cm in diameter and galvanized steel 0.6 cm in diameter²⁹. For conductors thinner than these values, the horizontal sag will be greater while for those thicker than these values the vertical sag will be greater. To first order, the equation for sag is given by $s = B_s wL^2/T$ where $w = f_y = mg$ is the weight of the cable, L is the length of the span, T is the tension, and B_s is a constant. From equation 1, we expect the horizontal drag force f_x to increase the tension by an amount proportional to u^2 , so that

$$s_x = B_s f_x L^2/T = B_A u^2 L^2/T \quad [3]$$

where B_A encapsulates all drag constants and cable properties. When s_x exceeds one half of the conductor separation, line-slap can occur. The example and values shown above demonstrate that horizontal sag exceeding $\frac{1}{2}$ conductor separation can occur at the design wind pressure for the conductor separation values specified in General Order 95, which start at 0.9 m for distribution lines.

While current regulations may not prevent line slap, it is not a common occurrence even during Santa Ana wind storms, though the Witch fire, California's fourth largest modern fire, was initiated by line slap from a 69 kV transmission line. As wind speed increases, one would first expect to see cases of line slap in cases where there is a combination of 1) conductors at minimum separation 2) thinner conductors 3) longer spans 4) more elastic conductor material and 5) topography promoting variable and chaotic wind conditions that cause conductors to swing out of phase with each other and 6) non-compliance with regulations. Cases in which a number of these factors have extreme values will be those for which line slap would be observed at the lowest wind speeds. We do not know the expected statistical distribution of these events. However, a statistical family having the correct asymptotic behavior and describing many extreme value problems is the Weibull distribution^{30,31}. Combining this distribution with Equation $s_x = B_s f_x L^2/T = B_A u^2 L^2/T$ [3]^c allows us to express the variation of line slaps with wind speed as:

$$N(s, u) = N_0 \exp\left(-\left(s / Bu^2\right)^\gamma\right) \quad [4]$$

To illustrate how strong a function of velocity this relation can be, if we take the example of $N(s, v)/N_0 = 10^{-5}$, if $\gamma = 1$, then a 10 % increase in u will increase the number of slaps by a factor of 7.4. If $\gamma = 2$, this increases to a factor of 40. It is likely that the statistical tail is truncated, since extreme cases may be observed by inspection and corrected.

Fatigue failures and wind speed

A third type of failure that can cause power line fires is when objects related to or near the conductor become fatigued and fail, allowing the conductor to come into contact with conductive or high-impedance objects. A huge variety of components make up an electrical distribution network, not to mention surrounding objects, made of a wide variety of materials and under a wide variety of stress and strain conditions. The relevant question in regard to wildland powerline fires is once fatigue failures causing fires begin to appear, how do we expect them to increase as a function of wind speed?

Principles of fatigue failure lead to the expectation that a combination of two effects will contribute to near-threshold failures: first that some components will have experienced an extended lifetime of stress-strain fluctuations and that the high-stress or strain conditions associated with extreme wind events will cause them to reach the end of their lifetime, and

another contribution from components that have degraded into a non-elastic condition due to environmental factors (corrosion, physical damage, high temperature, etc.) and which will fail within a small number of stress-strain cycles once the strain is raised above a threshold. In either case, we may use a strain life relation to derive a proportionality between probability of failure for an ensemble of similar objects at different points in their fatigue lifecycles^c:

$$P(u) \sim u^{-2/b} \quad [5]$$

where b is 0.5-0.7 for most metals. As in the previous section, the rate at which failures increase with wind speed will depend strongly on the statistical distribution of material properties and stresses throughout the electrical network. It might be expected that these might be best represented as extreme value statistics such as the Weibull distribution. This would yield a result

similar to equation
$$N(s, u) = N_0 \exp\left(-\left(s / Bu^2\right)^\gamma\right) \quad [4]:$$

$$N(u) \approx N_0 \exp\left(-\left(u^{-2/b}\right)^\gamma\right) \quad [6]$$

As in the case of line slap, a relation of this type would indicate that the number of faults and ignitions would increase very rapidly with wind speed once they begin to appear.

DISCUSSION

Southern California was hit by two conflagrations within four years. In the 2003 event, none of the major fires was attributable to power lines, whereas in the 2007 event, nine out of the 16 fires larger than 100 acres has been officially or unofficially attributed to power lines. The difference between these events is clear: wind speeds were much higher in 2007 than in 2003. Averaging three weather stations in San Diego county (Ammo Dump, Potrero, and Julian), peak gusts in the 2003 event averaged 33 mph (15 m/s), whereas in 2007 they averaged 59 mph (26 m/s). The increase in line faults coupled with reduced suppression efficiency due to rapid fire growth under high wind conditions is responsible for the greater number and destructiveness of power line fires under high wind conditions.

The great variety of electrical network components and surrounding environment make it impossible to construct a formal model of power line fires. However, by examining the physical processes and statistical considerations that apply to these systems, it is possible to set some constraints on how we expect the number of power line fires to increase with wind speed. One general conclusion that can be reached is that the number of fires will grow with a greater than linear dependency on wind speed, possibly much greater than linear. If wind gusts greatly exceeding design limits were to strike the network they would cause a myriad of ignitions, which under those conditions would lead to catastrophic consequences. Wind events with multiple power line ignitions, such as that of October 2007, provide an indication of the threshold for the rapid increase in ignitions with increasing wind speed.

One disturbing fact is that current California design guidelines allow for design wind loadings less than those observed in Santa Ana wind storms. This and other regulations affecting fire safety require urgent review. The design paradigm for electrical networks in wildland fire risk areas needs to change to accommodate return levels for extreme wind events in the 200+ year range, in the same way that California now designs for earthquake risks. Other remedial actions could include greater clearance requirements for conductors, and requiring spacers on all long spans to prevent line-slap.

A controversial measure now being implemented by some utilities consists of selectively turning off power to high-risk areas during severe events. While removing power line fire ignition risk, this measure may increase overall fire risk in by hampering communications, fire-fighting, and evacuation. Applying such a measure in a manner to maximize public safety requires careful study and review.

One measure that would further academic, governmental and industrial abilities to analyze the power line fire threat would be to require that all privately owned utilities make their fire, outage, and maintenance records publicly available. This would permit vulnerabilities to be detected before they are “found” by the next Santa Ana wind event. While California has a significant exposure to catastrophic power line fires, it is not unique in this regard. Lessons learned here will have global applicability in all environments where wind-driven wildland fires are a concern.

Acknowledgements

The author would like to express appreciation to David Sapsis and Cal Fire for providing CARS ignition data and to Patrick Pagni, Carlos Fernandez-Pello and Max Moritz for their comments and suggestions.

REFERENCES

¹ California Department of Forestry and Fire Protection; Percent of Fires by Cause, Statewide 5-Year Average (2000-2005); CDF Jurisdiction;

http://www.fire.ca.gov/about_factsheets.php/incidentsandevents_106_2000-2005.pdf, downloaded 12/12/2006.

² California Department of Forestry and Fire Protection; 20 Largest California Wildland Fires (by Acreage Burned / by Structures Destroyed)

http://www.fire.ca.gov/communications/downloads/fact_sheets/20LACRES.pdf

http://www.fire.ca.gov/communications/downloads/fact_sheets/20LSTRUCTURES.pdf ;

downloaded 2/17/2008; *Witch and Rice fires have since been attributed to power lines by Cal Fire; the Slide fire was attributed to power lines in press reports and is still under investigation by the US Forest Service*

³ OSFM, CDF, USFS, PG&E, SC Edison, SDG&E; Power Line Fire Prevention Field Guide; Mar 27, 2001; p. 1-5.

⁴ California Department of Forestry and Fire Protection; Fire Perimeters; FRAP program; <http://frap.cdf.ca.gov/data/frapgisdata/download.asp?spatialdist=1&rec=fire> ; downloaded 7/9/2008.

⁵ Malamud, B. D., G. Morein, and D. L. Turcotte (1998), Forest fires: An example of self-organized critical behavior; *Science* 281:1840-1842.

⁶ Moritz, Max A., et. al; Wildfires, complexity, and highly optimized tolerance; *Proceedings of the National Academy of Sciences of the United States of America*; December 13, 2005; 102: 17913.

⁷ Carlson, J. M. and John Doyle; Complexity and robustness; *PNAS* (2002) 99: 2538-2545.

⁸ Boer, Matthias M, et al.; Spatial scale invariance of southern Australian forest fires mirrors the scaling behaviour of fire-driving weather events; *Landscape Ecol* (2008) 23:899–913.

⁹ Albini, FA; Transport of firebrands by line thermals; *Combust Sci Technol* (1983) 32:277–88.

¹⁰ Woycheese JP, Pagni PJ, Liepmann DP. Brand lofting from large scale fires. *J Fire Prot Eng*

(1999) 10:32–44.

¹¹ United States Forest Service/California Department of Forestry (USFS/CDF); The 2003 San Diego county fire siege fire safety review; 2003; p. 15.

¹² R. Anthenien, S. Tse, and A.C. Fernandez-Pello; On the Trajectories of Embers Initially Elevated or Lofted by Ground Fire Plumes in High Winds; *Fire Safety Journal* (4/2006) 41: 349-363.

¹³ Keeley, J.E. and C.J. Fotheringham; Impact of past, present and future fire regimes on North American Mediterranean shrublands; 2003. In T.T. Veblen, W.L. Baker, G. Montenegro, and T.W. Swetnam (eds.), *Fire and Climatic Change in Temperate Ecosystems of the Western Americas*; Springer-Verlag; New York; pp.218-262.

¹⁴ California Department of Forestry and Fire Protection; CARS database; 1998-2008; provided as a courtesy.

¹⁵ Raphael, M. N.; The Santa Ana Winds of California; *Earth Interactions* (2003) 7:1-13.

¹⁶ National Wildfire Coordinating Group; National Fire Danger Rating System; Weather Station Standards; PMS 426-3; May 2005. More information is at <http://www.fs.fed.us/raws/>.

¹⁷ California Department of Forestry and Fire Protection; Fire Perimeters; FRAP program; <http://frap.cdf.ca.gov/data/frapgisdata/download.asp?rec=fthrt>; downloaded 2/7/2007.

¹⁸ Mesowest; The University of Utah Department of Meteorology; *provides graphical interface to weather station data archives*; <http://www.met.utah.edu/mesowest/>

¹⁹ California Public Utilities Commission; Application Proceeding A.06-08-010; Sunrise Powerlink Transmission Line Project; Mussey Grade Road Alliance (MGRA); MG-1; MGRA Phase 1 Direct Testimony and Phase 2 Direct Testimony; 2007-2008; Available at http://www.mbartek.com/cpucspl/cpuc_index.html.

²⁰ Ibid; MGRA Phase 1 Testimony; Appendix A; pp. 9-13.

²¹ Ibid; MGRA Phase 2 Testimony; Appendix 2D; pp. 7-11.

²² Tse, Stephen D. and A. Carlos Fernandez-Pello; On the Flight Paths of Metal Particles and Embers Generated by Power Lines in High Winds - a Potential Source of Wildland Fires; *Fire Safety Journal* (1998) 30:333-356.

²³ Flemmer RLC, Banks CL. On the drag coefficient of a sphere; *Powder Technol.* (1986) 48:217–21.

²⁴ Public Utilities Commission of the State of California; General Order Number 95; Rules for Overhead Electric Line Construction; Rev. Jan. 2006; Rule 43.

²⁵ Ibid; Rule 38.

²⁶ Ibid.

²⁷ Tse and Fernandez-Pello.

²⁸ CPUC General Order 95; Appendix C; p. C-6.

²⁹ Ibid; Appendix B; pp. B-3 – B-8.

³⁰ Weibull, W.; A Statistical Distribution Function of Wide Applicability; *ASME Journal of Applied Mechanics*; Sept. 1951; pp. 293-297.

³¹ Coles, S.; *An Introduction to Statistical Modeling of Extreme Values*; Springer; 2001; pp. 46-47.

APPENDIX – DERIVATION OF VELOCITY DEPENDENCE OF IGNITION SOURCES

Nomenclature

Variable	Definition	Units
\bar{u}	Wind velocity	m/s
A	Cross-sectional area	m ²
ρ_{air}	Air density	kg/ m ³
C_d	Drag coefficient	
\bar{F}_d	Drag Force	N
k	Spring constant	N/m
L	Conductor length	m
s	Conductor sag	m
T	Tension	N
d	Line clearance distance	m
$\Delta\varepsilon$	Strain amplitude	
σ'_f	Fatigue strength coefficient	Pa
E	Young's modulus	Pa
ε_f	Fatigue ductility coefficient	
b	Fatigue strength exponent (-0.05 to -0.12 for most metals)	
c	Fatigue ductility exponent (-0.5 to -0.7 for most metals)	

Elastic extension and conductor contact

One would expect that application of a cleared distance around the conductors, combined with routine maintenance would result in a threshold velocity v_0 below which no conductor-object contacts are observed, and a corresponding minimum elastic constant k_{min} . Likewise, one would assume that the density per unit area $\lambda(k)$ of identical objects with $k_{min} + \delta k > k > k_{min}$ to be constant with respect to linear distance from the conductor. Hence the number of conductor-object contacts for values of k in this region would vary as u^2 in accordance with Hooke's law in combination with Equation 1. As the wind speed increases, smaller values of k will be enabled to make line-conductor contact. We do not know the distribution $\lambda(k)$ – the distribution of elastic stiffness of objects near power lines. If we take the reasonable example of a flat distribution in k ($\lambda(k)=K$), the total number of line contacts would be expected to be:

$$N = L \int_{k_{min}}^{k_{max}} \lambda(k) dk = LK(k_{max} - k_{min}) = \frac{LKC}{d}(u^2 - u_{min}^2) \quad [7]$$

where C is a constant containing the aerodynamic drag constants, L is the length of the line segment, the clearance distance from the line is d , k_{max} is the maximum spring constant for which an object can extend by d , and u_{min} is the velocity at which an object with spring constant k_{min} will extend a distance d .

Line Slap

A statistical family having the correct asymptotic behavior for line slap and describing

many extreme value problems is the Weibull distribution, whose cumulative form is:

$$G(x) = 1 - \exp\left[-(x/\beta)^\alpha\right] \quad [8]$$

where $\alpha, \beta > 0$. For a value of horizontal line sag $x = s$, assume we have $N(s)$ line slaps out of a total population of N_0 conductor spans. The scaling factor β determines how far x varies from the mean – how far out on the statistical tail it is. Hence, one can express β as a function of the mean sag s_{mean} , and $s_{mean} \sim f_x$. So by Equation $s_x = B_s f_x L^2/T = B_A u^2 L^2/T$
 $[3, \beta = B_\beta u^2$, where B_β subsumes the other variables. The number of line slaps can then be expressed

$$N(s, u) = N_0 \exp\left(-\left(s/B_\beta u^2\right)^\alpha\right) \quad [9]$$

Fatigue failure

In metals, the relation between cyclic strain and the fatigue life is³²:

$$\frac{\Delta\varepsilon}{2} = \frac{\sigma_f'}{E} (2R)^b + \varepsilon_f' (2R)^c \quad [10]$$

For cyclic stress, the relation is similar, with the exception that the plastic fatigue term $\varepsilon_f' (2N)^c$ is replaced by fatigue limit – the stress below which failures are not observed to occur. Miner's rule allows us to separately sum cycles occurring at different stress magnitudes. Assuming that we do not know how far an arbitrary component has progressed along its failure curve, we can express the probability that a failure occurs during a given time interval t that a given stress or strain is operative as $P(t) = R_t/R$ where $R_t = \omega t$, ω being the mean load oscillation rate. We expect both stress and strain to be proportional to applied force, so $\Delta\varepsilon/2 \sim u^2$. Solving a single power law relation for the plastic regime allows us to invert Equation 6, showing that the failure probability is

$$P(u, t) \sim \omega t u^{-2/\gamma} \quad [11]$$

where γ is either b or c for the elastic and plastic regimes, respectively, yielding exponents in the range of 3-4 in the plastic regime ($N \ll N_t = 1/2(\varepsilon_f' E / \sigma_f')^{1/(b-c)}$) in which most failures would be expected to occur.

³² Dieter, George E.; Mechanical Metallurgy; McGraw-Hill; San Francisco; 1986; pp. 375-394.